A numerical simulation of photothermal response in laser medicine

Xiaoxia Li (李小霞), Shifu Fan (范世福), Youquan Zhao (赵友全), and Songshan Xiao (肖松山)

College of Precision Instrument, Tianjin University, Tianjin 300072

Received November 4, 2003

In this paper, we reported a numerical solution of laser induced thermal effect in the bio-tissue. The model of photothermal effect and classical Pennes bio-heat transfer equation were introduced. Finite element method (FEM), which was realized by Matlab software, was used to calculate the temperature distribution. He-Ne laser (633 nm) was used to simulate the physical therapy in *in vivo* skin tissue. Under the cylinder coordinates, the three-dimension (3-D) geometry of tissue was reduced to two-dimension (2-D) computation. The results contained the radial, axial and temperature 3-D color plot. Combining the time animation display was possible. By changing the laser and tissue parameters we can get different results. This will be the initial and indispensable work of the non-destructive evaluation of the laser induced injury.

OCIS codes: 000.4430, 140.3330, 350.5340, 270.3430.

In 1948 Pennes introduced the bio-heat transfer equation for the first time, which was later proved to be very applicable[1]. Weinbaum and Jiji developed it in 1985 by replacing thermal conductivity K in Pennes's Equation with an effective thermal conductivity K_{eff}, which was more accurate in the tissues with small blood vessels $(50-200)$ μm[2] and fast blood flow. In the He-Ne laser clinic application, the Pennes's Equation is more proper because the power density is low and the arterial temperature can equilibrate thermally "instantaneously" with the surrounding tissue temperature.

The experimental results were limited because the temperature measuring technology used in living organism was limited from the invasive injury and number tolerance. Therefore numerical computation is called for medical thermal computation. Finite different technique (FDT)[3,4] and finite element method (FEM)[5] are two usually used solutions to solve bio-heat transfer problem. But to reduce the computation difficulty, most computations have cut the blood perfusion term[4,5] or only calculate one-dimension distribution[6]. In fact, many commercial softwares such as matlab, heating, and ansys, RadTherm of thermoanalytics etc. have now come into use to solve the complex partial differential equation. Unluckily those softwares, which originally aimed at engineering heat transfer, are difficult to be directly used in the bio-heat transfer equation. FEM with Matlab is selected because FEM can be adaptable to arbitrary geometry, and the Matlab source programs are almost open to the users and are convenient be to rewritten to specific application. The tissue optical and thermal properties should be selected correctly. Laser source term, boundary condition, and initial condition should also be carefully considered in the solution of the bio-heat transfer model.

Modeling of photothermal process is generally conducted in three steps: 1) calculation of light distribution; 2) calculation of temperature rise; 3) calculation of the extent of the thermal damage. Figure 1 is a tissue thermal model.

The S (source), T (temperature) and Ω (damage value) are all the function of r, z and t.

The classical Pennes bioheat transfer equation is used in our simulation

$$\rho C\frac{\partial T}{\partial t} = K\nabla^2 T + Q_{\text{m}} + Q_r + W_{\text{b}}C_{\text{b}}(T_{\text{b}} - T), \qquad (1)$$

where ρ is tissue density, C is tissue specific heat, K is thermal conductivity of tissue, Q_{m} is metabolic rate, which is usually neglected because it is trifle comparing with laser source, Q_r is laser source, W_{b} is the blood perfusion rate, C_{b} is the specific heat of blood, T_{b} is the temperature of artery, T is the temperature of tissue, and t is calculation time. Equation (1) will be solved by FEM.

Figure 2 shows the geometry of tissue.

The considered tissue space is divided into many triangles. When these triangles are small enough, the temperatures of these triangles' points which were looked as homogeneous can represent the temperature distribution.

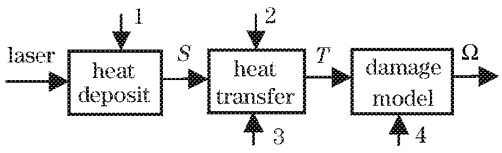

Fig. 1. Photothermal effect model. 1: optical properties of laser and tissue; 2: heat properties of tissue; 3: boundary condition; 4: damage ration coefficient.

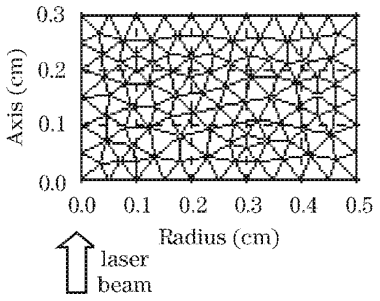

Fig. 2. Geometry of tissue under cylinder coordinates.

The surface is natural convective boundary

$$-K \cdot \vec{n} \cdot \nabla T = h(T - Te), \quad z = 0, \tag{2}$$

where the surface convective heat transfer coefficient h is selected as 4.0×10^{-4} W·cm^{-2}·K^{-1}, the environmental temperatures is 23 °C. *In vivo* the bottom and right side is constant temperature boundary

$$T_0 = 37°\mathrm{C}, z = 0.3 \text{ cm and } r = 0.5 \text{ cm}, \tag{3}$$

the cylinder axis is insulated boundary

$$\vec{n} \cdot \nabla T = 0 \quad r = 0, \tag{4}$$

the initial condition is

$$T_0 = 37 \text{ °C}. \tag{5}$$

Under the symmetry cylinder coordinate the Gaussian laser source is[6]

$$Q_r(r,z,t) = -\mathrm{d}I/\mathrm{d}z$$

$$= [\mu_t + 0.5\mu_s(r/w(z))^2]I(r,z,t), \tag{6}$$

$$I(r,z,t) = (1-R)I_0 \exp[-0.5(r/w(z))^2]$$

$$\times \exp(-\mu_t z)\exp[-4(t-\tau)^2/\tau^2], \tag{7}$$

where $R = 0.05$ is the mirror reflectivity, I_0 is the fluence rate, $w(z) = w_0 \exp(-0.5\mu_s z)$, ω_0 is the radius of laser beam when the intensity decays to 1/e. $\mu_t = \mu_s + \mu_a$, μ_s is the tissue scattering coefficient, and μ_a is the tissue absorption coefficient.

During the simulation, human skin is supposed to be irradiated by He-Ne laser. The used *in vivo* parameters are listed in Table 1. The tissue density $\rho = 1.3 - 0.3w$, the water content of skin $w = 20\%$, heat specific $C = 4.19(0.37 + 0.63w/\rho)$, thermal conductivity $K = 4.19(0.133 + 1.36w/\rho)$[7], absorption and scattering coefficient μ_a, μ_s were of human skin dermis[8]. Blood perfusion rate W_b is of human skin[9], heat specific C_b is calculated as the same as the tissue, the water content of blood is 78.7%.

The numerical simulation results are given in Figs. 3 – 6. Figure 3 shows the 3-D temperature of both radius and axial coordinates. The results allow animation 3-D display with time. So the dynamic temperature rise procedure can be clearly seen.

Figure 4 shows the temperature rise versus cure time with different power density and different depth at the radial center. The temperatures all rise to a stable status after about 100 s and then stop to rising. Besides other factors, if the temperature is proper the cure time can be expanded to any wanted length. Except special request, the common usage surface temperature should not exceed 43 °C, which is the tolerate limit of human. So from Fig. 4(a), the power density should not higher than 60 mW/cm^2. This is well consistent with the clinic application[10]. Figure 4(b) shows the temperature of 0.1 cm under the surface center decrease rather fast. Even in the case of 80 mW/cm^2, the temperature was not above 41 °C.

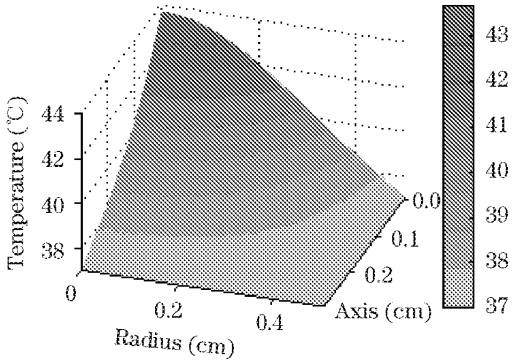

Fig. 3. The three dimention (3-D) temperature plot at I = 80 mW/cm^2 and time = 600 s.

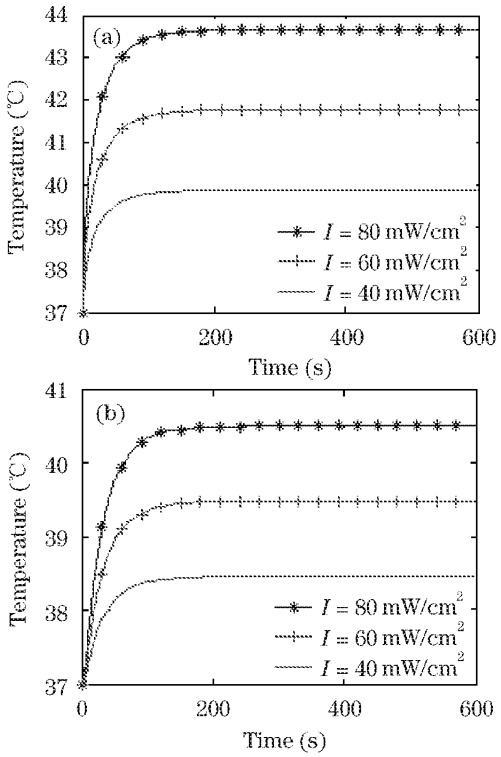

Fig. 4. The temperature versus cure time plots at radial center. (a) r = 0 cm, z = 0 cm; (b) r = 0 cm, z = 0.1 cm.

Table 1. Calculaing Parameters in the Bio-Heat Transfer Equation

Laser					Human Skin					Blood		
λ	I_0	w_0	τ	Step	μ_s	μ_a	ρ	C	K	W_b	C_b	T_b
nm	mW/cm^2	cm	min	s	cm^{-1}	cm^{-1}	g/cm^3	J/(g·°C)	mW/(cm·°C)	ml/(g·s)	J/(g·°C)	°C
633	40 – 80	0.25	10	1	180	0.7	1.24	1.98	1.48	9×10^{-3}	3.5	36.5

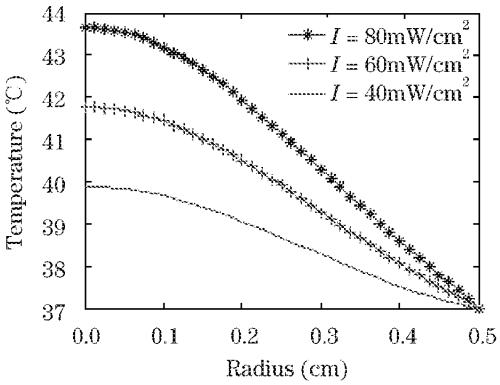

Fig. 5. The radial temperature plot at $z = 0$ cm.

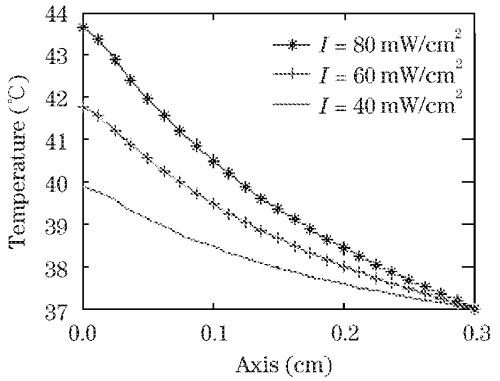

Fig. 6. The axial temperature plot at $r = 0$ cm.

Figures 5 and 6 are the stable radial temperature response at the surface and the stable axial temperature response at the radial center. We can see the radial temperature is Gaussian shape, which is the result of the Gaussian laser beam. And the axial temperature decreases exponentially with depth because the source decreases exponentially. So the temperature distribution obeys almost the same rule of source, which was determined by the laser and tissue optical parameters.

The tissue thermal parameters will influence the heat transfer characteristics too. Figure 6 shows the skin tissue is heat conduct resistant matter.

Though most researches look the physical therapy of He-Ne laser as non-thermal effect and usually overlook the temperature effect on the curative effect, we believe most bio-stimulations are close with temperature. From the results we can clearly see the temperature response under different laser power density. The doctors should be glad to see such results and to guide their treatments at different cases. In recent years, the combination of hyperthermia and photodynamic therapy (PDT) as cancer treatment has aroused interest[3]. For more knowledge of the relation of temperature and physical therapy, we needs further biology study in this field. This numerical computation will be useful to quantitative study in laser medicine.

Exact simulation depends on the correct optical and thermal properties of tissue and the laser optical parameters. Because these properties of even the same kind of tissue vary with place and individual, up to now the systemic properties of tissue, especially in *in vivo* human tissue are not easy to measure or calculate. As a common simulation, this numerical computation is ready to change with the parameters and to develop with new data of tissues and lasers.

This work was supported by Tianjin Natural Science Foundation under Grant No. 023602611. X. Li's e-mail address is xiaoxialee@twtmail.tju.cn.

References

1. H. H. Pennes, J. Appl. Phys. **1,** 93 (1948).
2. S. Weinbaum L. and M. Jiji, ASME J. of Biomechanics Engineering **106,** 331 (1985).
3. C. Sturesson and S. Andersson-Engels, Phys. Med. Biol. **40,** 2037 (1995).
4. S. S. Xie, H. Q. Yang, and B. H. Li, J. Optoelcetron. ·Laser (in Chinese) **12,** 746 (2001).
5. S. H. Diaz, G. Aguilar, E. J. Lavernia, and B. J. F. Wong, IEEE J. Sel. Top. in Quantum Electron. **7,** 944 (2001).
6. Z. M. Li, J. Optoelcetron.·Laser (in Chinese) **11,** 431 (2000).
7. A. J. Welch, IEEE J. Quantum Electron. **20,** 1471 (1984).
8. A. Roggan, J. Beuthan, S. Schruder, and G. Muller, Diagnostik and Terapie met dem Laser Phys. Bl. **55,** 25 (1999).
9. B. Lynn and B. Cotsell, Microvasc. Res. **41,** 197 (1991).
10. S. L. Yang, Y. Gu, and F. G. Liu, Modern Rehabilitation (in Chinese) **4,** 1382 (2000).